Effect of Absorbing Aerosol on Shortwave Radiative Forcing of Climate

S. Nemesure and S. E. Schwartz
Brookhaven National Laboratory
Upton, New York

Abstract

We have examined the optical and radiative properties of sulfate aerosol internally and homogeneously mixed with an absorbing substance and evaluated the dependence of forcing on controlling variables including the imaginary component of the index of refraction k, particle radius r, solar zenith angle (SZA), and surface reflectance R. For example, for an aerosol mixture of sulfate and absorber having r = 0.12 μm and k = 0.008 (corresponding to a single scattering albedo, ω = 0.9) with R = 0.15, the global-average (half the average over the illuminated hemisphere) normalized forcing (forcing divided by sulfate column burden) is $-575\,\mathrm{W/g(SO_4^{2-})}$ compared to $-800\,\mathrm{W/g(SO_4^{2-})}$ for pure sulfate aerosol (k = 0). We have mapped out the boundaries for which the forcing is negative (cooling) versus positive (warming). For example, for r = 0.12 μm and R = 0.15, the normalized global-average forcing is positive for $k \gtrsim 0.04$ ($\omega \lesssim 0.65$). Instantaneous normalized forcing becomes positive at even smaller values of k for the sun near zenith. Comparison with single scattering albedos measured at the Atmospheric Radiation Measurement (ARM) Southern Great Plains (SGP) site and elsewhere suggest that the sign of tropospheric aerosol forcing is predominantly negative.

Introduction

Radiative forcing of climate by sulfate aerosols is thought to exert a direct shortwave forcing of climate comparable in magnitude but opposite in sign to the longwave forcing by anthropogenic greenhouse gases. However, recent work has questioned the cooling influence of aerosols because of possible influences of absorbing aerosol that might offset the negative forcing of a purely scattering aerosol.

To examine the decrease of magnitude of direct shortwave radiative forcing by aerosols as a consequence of absorption, we have carried out calculations of this forcing for an aerosol with increasing amounts of absorption, and compared to the situation for a purely scattering aerosol as examined previously (Nemesure et al. 1995).

Approach

The following approach was used for our calculations:

- examine the influence of absorption on aerosol optical properties and on radiative forcing as a function of particle radius, SZA, and surface albedo
- increase aerosol absorption by increasing imaginary component of refractive index for particles treated as homogeneous spheres
- calculate influence of absorption on aerosol optical properties and radiative forcing.

Theory

The radiative forcing by an optically thin aerosol, per unit scattering volume (i.e., per unit area and unit vertical height, Δz), due to upward scattering of the direct solar beam is

$$\Delta F(\theta_0) = (F^{\downarrow} \cos\theta_0)(\alpha_{ext} \sec\theta_0)\omega\beta(\theta_0)C\Delta z$$

where $F^{\downarrow} = \cos\theta_0$ the incident direct beam flux at the top of the scattering element
θ_0 = SZA
α_{ext} = mass-extinction efficiency
ω = single-scattering albedo
$\beta(\theta_0)$ = upscatter fraction
C = mass concentration.

Note that sec cancels cos, so

$$\Delta F(\theta_0) = F^{\downarrow}\alpha_{ext}\omega\beta(\theta_0)C\Delta z$$

The extinction efficiency is the sum of the scattering and absorption efficiencies:

$$\alpha_{ext} = \alpha_{scat} + \alpha_{abs}$$

The single-scattering albedo is the ratio of the scattering to extinction efficiencies

$$\omega = \frac{\alpha_{scat}}{\alpha_{ext}} = \frac{\alpha_{scat}}{\alpha_{scat} + \alpha_{abs}}$$

so that

$$\Delta F(\theta_0) = F^{\downarrow}\alpha_{scat}\beta(\theta_0)C\Delta z$$

The upscatter fraction (Wiscombe and Grams 1976) is

$$\beta(\theta_0) = \frac{1}{2\pi}\int_{\frac{\pi}{2}-\theta_0}^{\frac{\pi}{2}+\theta_0} P(\theta)\sin\theta\cos^{-1}(\cot\theta_0\cot\theta)d\theta + \frac{1}{2}\int_{\frac{\pi}{2}+\theta_0}^{\pi} P(\theta)\sin\theta d\theta$$

Here P(θ) is the phase function normalized to

$$\int P(\theta)d\Omega = 4\pi$$

The hemispheric mean forcing taking into account multiple reflection between surface and aerosol is

$$\Delta F = -\frac{1}{2}F_0T^2\tau\bar{\beta}\omega\left\{(1-R)^2 - 2R(1-\omega)/\bar{\beta}\omega\right\}$$

where τ is aerosol optical depth, $\tau = \int \alpha_{ext}dz$, and R is the surface reflectance.

This leads to a critical single-scattering albedo ω* such that forcing is positive for ω < ω*

$$\omega^* = \frac{2R}{\beta(1-R)^2 + 2R}$$

For the index of refraction n = h – ik h, h was taken equal to 1.4, corresponding to $(NH_4)_2SO_4$ at 80% RH. and k was varied from 0 to 0.08 to introduce absorption. We treat the absorption index k as the "independent variable" of the calculation, rather than the single-scattering albedo ω, as is often customary. The reason for this is that the (complex) index of refraction is a property of the material; increasing the absorption index k while holding the scattering index h constant is equivalent to adding increasing amounts of absorbing material to a base-case sulfate material. (In contrast, the single-scattering albedo is not dependent only on composition but is a function also of particle radius.) This approach permits examination of the radius dependence of the effect of absorbing material on aerosol optical properties and radiative forcing.

A radiative transfer model "6-S" (Vermote et al. 1997) with five-point quadrature was used to calculate upwelling irradiance at the top of the atmosphere, $F_{TOA}^{\uparrow}$. Instantaneous forcing was evaluated as

$$\Delta F = F_{TOA}^{\uparrow}(\text{no aerosol}) - F_{TOA}^{\uparrow}(\text{aerosol})$$

(A negative ΔF is a cooling influence; positive warming.) Forcing was calculated for aerosol optical depth of 0.20 at 550 nm.

To permit immediate comparison with the case of scattering only, we express mass scattering and absorption efficiencies relative to sulfate mass in particle and forcing relative to sulfate mass in the column. Forcing is thus expressed as normalized forcing, that is forcing per sulfate mass in column $\Delta G = \Delta F / B_{SO_4^{2-}}$, where $B_{SO_4^{2-}} = \int C_{SO_4^{2-}} dz$; normalized forcing has units $Wm^{-2}/\left|g\left(SO_4^{2-}\right)m^{-2}\right|$ or $Wg(SO_4^{2-})$. Global average normalized forcing is evaluated as half the integral over the sunlit hemisphere. The normalized forcing for any given size distribution is evaluated as the integral of the normalized forcing at a given radius over the mass size distribution of the aerosol.

Results

The dependence of aerosol optical properties on absorption index k and radius is shown in Figure 1 for the range of particle radius, 0.03 to 1 μm, pertinent to climate forcing by anthropogenic aerosols. As k increases, α_{abs} exhibits an increase that is relatively independent of radius. At low radius, where scattering is inefficient, α_{ext} exhibits a strong increase whereas α_{scat} remains nearly unchanged. At larger radii, α_{scat} exhibits a slight decrease that almost compensates the increase in extinction due to absorption so that α_{ext} remains nearly unchanged. The single-scattering albedo also decreases with increasing k (see Figure 2). Note that the decrease is quite substantial for radius $\lesssim$ 0.1 μm. The range of values of k employed here yields values of ω that encompass the pertinent range of values exhibited by ambient nonurban aerosols, as measured at the ARM SGP site and elsewhere.

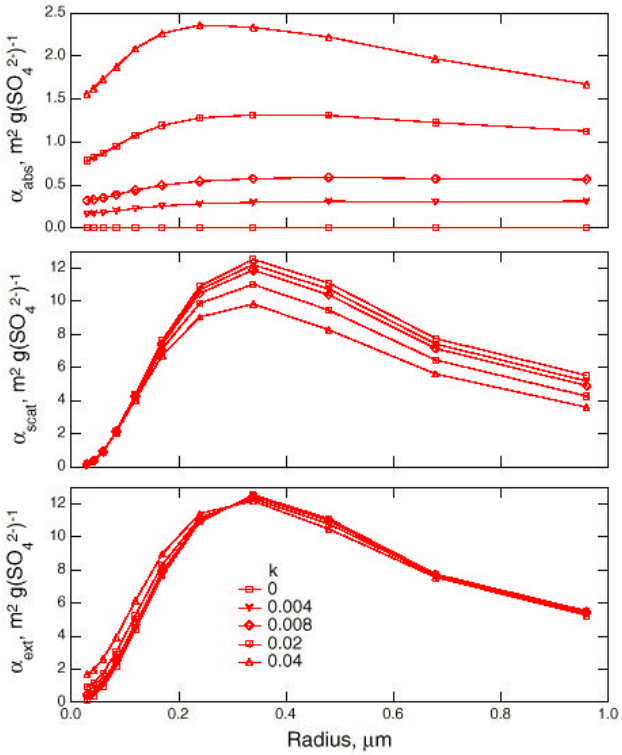

Figure 1. Dependence of absorption, scattering, and extinction efficiencies on radius and absorption index *k*. Calculations are for broadband shortwave weighted by solar intensity.

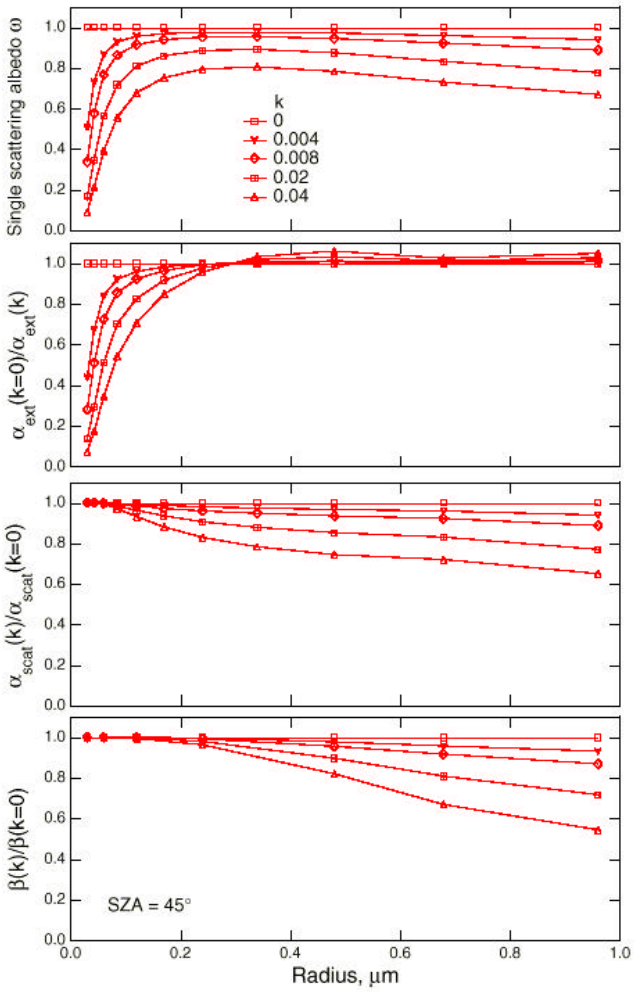

Figure 2. Dependence on particle radius and absorption index *k*, of single-scattering albedo, and of extinction and scattering efficiencies, and of upscatter fraction (for SZA 45°) relative to those for *k* = 0. Note that for extinction cross section α_{ext}, the ratio is given in the opposite sense. Calculations are for broadband shortwave weighted by solar intensity.

The values of α_{ext} and α_{scat} relative to those for the non-absorbing particle are shown in Figure 2. The extinction efficiency α_{ext} increases strongly with increasing k at low radius because of the low scattering efficiency; in the figure the ratio of α_{ext} (k) to α_{ext} (k = 0) is plotted in an inverse sense to show that the dependence on k almost exactly cancels the dependence of ω on k. Hence, the product $\omega\alpha_{ext}$, which is equal to α_{scat}, exhibits a much weaker dependence on k and r, especially at small radii, than either of the two factors. For this reason, it is more useful to consider the forcing a function of α_{scat} than of α_{ext} and ω. The decrease in scattering efficiency, which is appreciable throughout much the radius range, contributes to a decrease in shortwave forcing.

The dependence of upscatter fraction β on radius, absorption index, and μ_0, the cosine of the SZA, is shown in Figure 3. Note that the zenith angle dependence of the upscatter fraction characteristic of the nonabsorbing particles is exhibited also for the absorbing particles. For the larger particles there is an appreciable decrease of the upscatter fraction relative to that for the nonabsorbing particle; this is due to a relative increase in forward scattering, which in turn is attributed to relatively less absorption of forward scattered photons, which only graze the particle, than of back-scattered photons, which must traverse the bulk of the particle.

The ratio of upscatter fraction in the absorbing particle to that for the nonabsorbing particle is shown in Figure 2 for SZA 45°; the plots for other zenith angles are quite similar in shape and magnitude. For smaller radii there is little decrease in upscatter fraction, but at larger radii this decrease is appreciable, exerting a comparable contribution

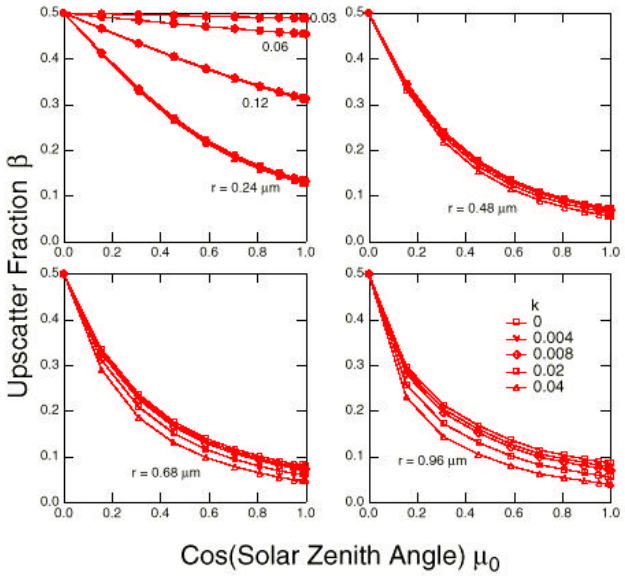

Figure 3. Dependence of upscatter fraction β on radius, absorption index, and μ_0, the cosine of the SZA. Calculations are for broadband shortwave weighted by solar intensity.

to the decrease in shortwave forcing to that due to decreased scattering efficiency.

The forcing calculated with the radiative transfer model is shown in Figure 4 as a function of particle radius and cosine of the SZA for several values of absorption index, all for surface albedo 0.15. Note that the shape of the dependence of forcing on radius and μ_0 is unchanged for increasing k, but that the magnitude decreases considerably for the range of values of k examined. At higher values of k, the forcing is seen to become positive (warming) especially at low SZA. Figure 5 presents the radius dependence of the global average forcing, again for surface albedo 0.15. Note that for all values of k the global average forcing is negative throughout much of the radius range, but that at higher values of k the forcing becomes positive, even in global average, for large radius and also for quite small radius.

Figure 5 also shows for comparison several representative aerosol size distributions (Nemesure et al. 1995) to permit comparison of the radius dependence of the forcing. Note the near coincidence of the peaks in the several size distributions with the maximum in magnitude of the global average normalized forcing.

Figure 6 shows the dependence of normalized forcing on absorption index k evaluated for the several size distributions

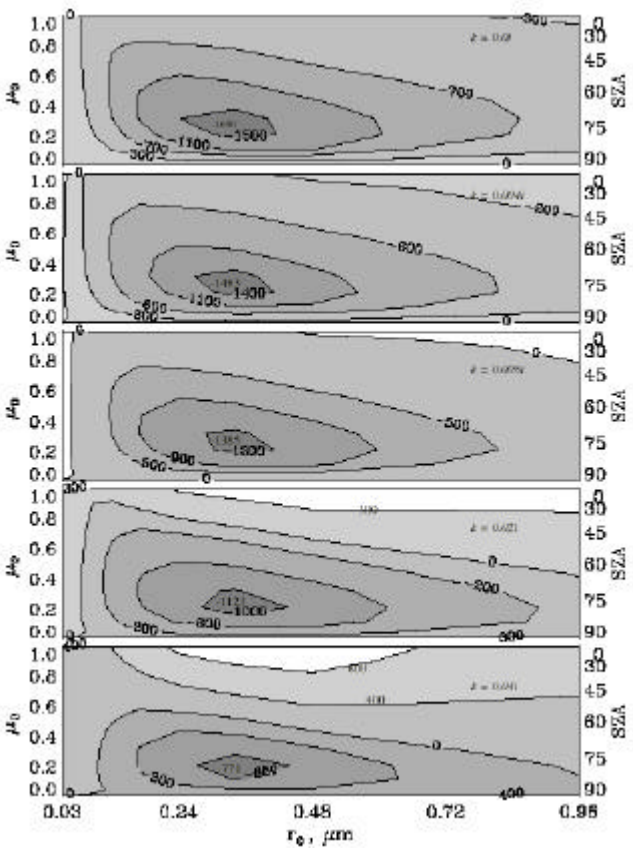

Figure 4. Instantaneous clear-sky broadband shortwave normalized radiative forcing y sulfate aerosol with internally mixed absorber, (ΔG) $Wg(SO_4^{2-})^{-1}$, as a function of particle radius and μ_0 = cos(SZA) over a surface with reflectance, R = 0.15, for several values of the absorption index k. The bold zero contour line partitions negative forcing (cooling) from positive forcing (warming).

and for a range of values for surface reflectance. The top axis gives the value of single-scattering albedo ω that corresponds to the value of k indicated on the bottom axis; note that this correspondence differs for the several size distributions. The forcing can be negative or positive depending on the absorption index and surface reflectance, the exact demarcation depending somewhat on the size distribution. Depending on the surface albedo there can be substantial reduction in the magnitude of negative forcing with increasing absorption index. Even more significant is the fact that the positive forcing can be quite high for high albedo of underlying surface. Examples of such high albedo situations would include aerosol over snow or clouds.

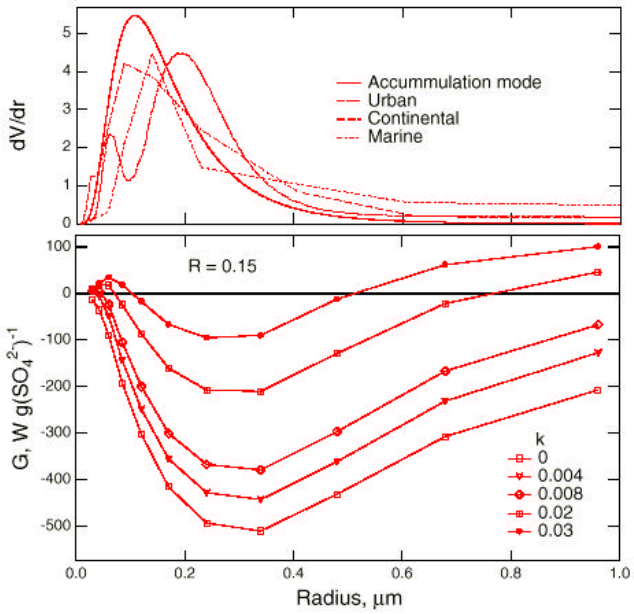

Figure 5. Global average clear-sky broadband shortwave normalized forcing by sulfate aerosol with internally mixed absorber as a function of radius, for several values of the absorption index *k* over a surface with reflectance *R* = 0.15. The top panel shows several aerosol volume size distributions. The zero line divides positive and negative forcing.

Conclusions

- The magnitude of aerosol negative forcing is highly sensitive to absorption in the particle size range of representative anthropogenic aerosols.
- The sign of aerosol forcing becomes positive only for high surface albedo, such as over clouds and snow.
- A manuscript is in preparation. For further information contact ses@bnl.gov.

References

Nemesure, S., R. Wagener, and S. E. Schwartz, 1995: Direct shortwave forcing of climate by anthropogenic sulfate aerosol: Sensitivity to particle size, composition, and relative humidity. *J. Geophys. Res*., **100**, 26,105-26,116.

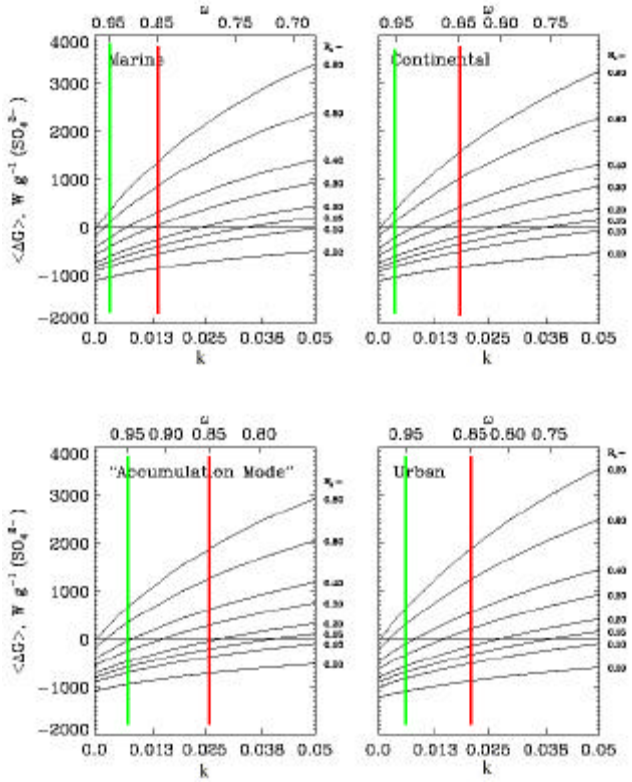

Figure 6. Global average clear-sky broadband shortwave normalized sulfate forcing as a function of absorption index *k* for several values of the surface reflectance. The zero line divides positive and negative forcing. Red and green lines represent bounds of typical range of single-scattering albedos at SGP. (For a color version of this figure, please see *http://www.arm.gov/docs/documents/technical/conf_9803/nemesure-98.pdf*.)

Vermote, E. F., D. Tanre, J. L. Deuce, M. Herman, and J.-J. Morcrette, 1997: Second simulation of the satellite signal in the solar spectrum, 6S: An overview. *IEEE Trans. Geosci. Rem. Sens*., **35**, 675-686.

Wiscombe, W., and G. Grams, 1976: The backscattered fraction in two-stream approximations. *J. Atmos. Sci*., **33**, 2440-2451.